Multi-speed operation of single-phase induction motor using a naturally commutated triac

M.Y. Abdelfattah [a], A. El-Zawawi [a] and A.M. Ibrahim [b]
[a] *Electrical Eng. Dept., Faculty of Eng., Alexandria University, Alexandria, Egypt*
[b] *Abu-Kir Fertilizer Co., Alexandria, Egypt*

Single-phase induction motors, like poly-phase induction motors, have a nearly constant speed characteristic. Many methods are used to control these motors. In this paper a new method for speed control is presented for controlling such motors. The method used employs, only, a naturally commutated triac placed in the supply line. The triac is controlled for both variable frequency and variable voltage operation to prevent saturation from becoming excessive. Variation of frequency is obtained by using ring-tail counter (Johnson counter) circuit which implements integral-cycle control technique to obtain the required fundamental frequency. Variation of voltage is obtained by using a phase control delay circuit. A mathematical model based on symmetrical components is proposed for digital simulation of the machine. The proposed system was validated experimentally and comparison is made between theoretical and experimental results.

تعتبر المحركات الحثية أحادية الطور ذات سرعات ثابتة تقريبا مثلما هو الحال بالنسبة للمحركات الحثية ثلاثية الطور. هناك طرق عديدة للتحكم في مثل هذا النوع من المحركات. يقدم هذا البحث طريقة جديدة للتحكم في سرعة المحركات الحثية أحادية الطور. الطريقة الجديدة تعتمد على استخدام نبيطة ترياك واحدة تعمل بنظام التبديل الطبيعي متحكم فيها للتحكم في تردد المصدر المغذي لمحرك حثي أحادي الطور وفي ذات الوقت التحكم في الجهد المغذي للمحرك وذلك لمنع ظاهرة التشبع. وقد تم تغيير التردد باستخدام عداد جونسون الذي يستخدم مبدأ تحكم الدورة المتكامل للحصول على التردد المطلوب. أما تغير الجهد فقد تم باستخدام مبدأ التحكم الوجهي. ويقدم البحث تحليلا رياضيا للآلة مبنيا على المركبات المتماثلة لدراسة خواص الآلة. تم إجراء التجارب المعملية للحصول على نتائج ومقارنتها بالنتائج النظرية.

Keywords: Single-phase induction motor, Multi-speed operation, Integral-cycle control

1. Introduction

Single-phase induction motors are mostly built in the fractional horse-power range. These motors are used for many types of equipment in homes, offices, shops, and factories. Single-phase induction motors, like poly-phase induction motors, have a nearly constant speed characteristic.

Many methods are used to control these motors. Controlling the applied voltage to the machine is considered the most common technique [1-5]. The main drawback of such a technique is the reduced starting and breakdown torque capability, making it suitable for fans or similar centrifugal loads. Also, for this method of speed control the slip increases at lower speeds, making the operation inefficient.

Another technique used for the speed control of the machine employs a chopper circuit in the stator side [6]. The chopping switch is placed across a diode rectifier bridge, which terminates the stator winding from the opposite side to the supply. This technique is considered as a non-conventional cycloconverter. There is no need for a dc bus capacitor. The good thing about this technique is that changing the frequency is followed by a reduction in the rms value of applied voltage to the machine terminals. This technique provides an intermediate range of speed variation. Fig. 1 shows a schematic diagram for the dc chopper-fed drive reported in ref. [6].

More complex and expensive techniques used for adjustable speed single-phase induction motor drives are those of PWM strategies. Among them, the most widely used,

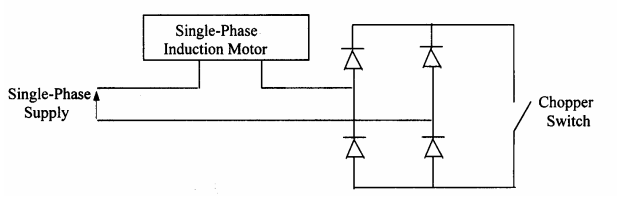

Fig. 1. DC chopper-fed single-phase induction motor.

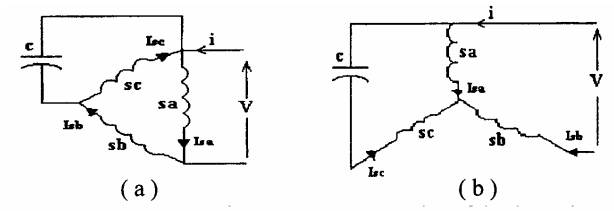

Fig. 2. Stator connections for single-phase operation of the three-phase induction motor.

are sinusoidal PWM and Space Vector PWM (SVPWM) techniques [7-10].

In the present paper a new scheme is suggested to control the machine. It is considered as a modification for the previous work presented in ref. [6]. Only one naturally commutated triac is placed in the supply line. Here, the firing circuit used will fulfill two requirements: (i) Changing the frequency of the applied voltage to the motor (integral cycle control), and (ii) Changing the applied voltage to the motor(phase angle control). The reason for this is to prevent saturation from becoming excessive and probably damaging the machine. A mathematical model based on symmetrical components is proposed for digital simulation of the machine [11].

A three-phase induction motor can be operated from a single-phase supply system using a capacitor, by connecting the stator windings as shown in fig. 2. This connection was used to provide adequate basis of comparison with the results of ref. [6]. The connection shown in fig. 2-a applies to a delta-connected motor; while that shown in fig. 2-b is suitable for a star-connected motor; where s_a , s_b , and s_c represent the three stator windings and C is the capacitor.

The proposed system was validated experimentally and comparison is made between theoretical and experimental results.

2. The mathematical model

Here, the instantaneous symmetrical components technique is used to analyze the machine operation. The instantaneous, power invariant, three-phase symmetrical components transformation is given by:

$$[c] = \frac{1}{\sqrt{3}} \begin{bmatrix} 1 & 1 & 1 \\ a^2 & a & 1 \\ a & a^2 & 1 \end{bmatrix} . \quad (1)$$

Where,

$$a = e^{j2\pi/3} .$$

The instantaneous symmetrical components for the three-phase quantities u_a, u_b, and u_c are:

$$[u]_{abc} = [c]\,[u]^{\pm 0}. \quad (2)$$

Where:

$$[u]_{abc} = [u_a \quad u_b \quad u_c]^T \quad , \quad (3)$$

$$[u]^{+-0} = [u^+ \quad u^- \quad u^0]^T \ , \quad (4)$$

where u^+, u^- , and u^0 are the positive, negative and zero sequence quantities, respectively, and T denotes the transpose. For the stator connections shown in fig. 2, zero sequence quantities are absent. Furthermore, the negative sequence quantities are always complex conjugates of the corresponding positive sequence quantities. Thus, only the positive sequence quantities are required for the complete solution.

The positive sequence operational equivalent circuit of three-phase induction motor is as shown in fig. 3 [11]. In this circuit R_s and X_{ls} are the per phase resistance and leakage reactance of the stator; R_r and X_{lr} are the per phase rotor resistance and leakage reactance referred to stator, and X_m is the magnetizing reactance. V and I refer to voltages and currents, subscripts s/r refer to stator/rotor. The operator $p = (1/\omega)d/dt$; where ω is the base supply radian frequency, υ is the p.u. speed with synchronous speed as base speed. All rotor quantities are referred to stator.

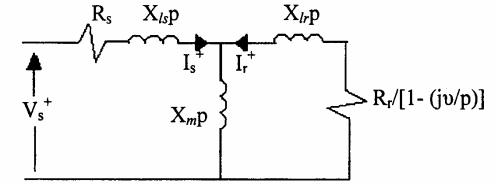

Fig. 3. Operational positive-sequence equivalent circuit.

The equivalent circuit shown in fig. 3 can be justified as follows. The equations of the induction machine in terms of stationary (d-q) reference axes expressed in matrix form-with the operator p defined as $p = (1/\omega)d/dt$ - are:

$$\begin{bmatrix} \upsilon_{ds} \\ \upsilon_{qs} \\ 0 \\ 0 \end{bmatrix} = \begin{bmatrix} R_S + X_S p & 0 & X_m p & 0 \\ 0 & R_S + X_S p & 0 & X_m p \\ X_m p & X_m \nu & R_r + X_r p & X_r \nu \\ -X_m \nu & X_m p & -X_r \nu & R_r + X_r p \end{bmatrix} \text{x} \begin{bmatrix} i_{ds} \\ i_{qs} \\ i_{dr} \\ i_{qr} \end{bmatrix},$$

which is in the form $\mathbf{v} = \mathbf{Z}\,\mathbf{i}$. Using the transformation matrix,

$$\mathbf{C} = \frac{1}{\sqrt{2}} \begin{bmatrix} 1 & 1 & 0 & 0 \\ -j & j & 0 & 0 \\ 0 & 0 & 1 & 1 \\ 0 & 0 & -j & j \end{bmatrix},$$

to transform the impedance matrix $\mathbf{Z}$ to positive, negative, forward and backward axes, leads to :

$$\mathbf{Z}' = \mathbf{C}_t^* \mathbf{Z}\, \mathbf{C} \cdot$$

It can be shown that, viewed from the primary terminals, in terms of positive, forward axes, the machine appears as an impedance Z^+_s given by:

$$Z_S^+ = \frac{\upsilon_S^+}{I_S^+} = \frac{(R_S + X_S p)\left(\dfrac{R_r}{\left(1 - j\dfrac{\nu}{p}\right)}\right) - p^2 X_m^2}{\dfrac{R_r}{\left(1 - j\dfrac{\nu}{p}\right)} + p X_r}.$$

If this is expressed in terms of X_{ls} and X_{lr}, defined by the equations:

$X_s = X_{ls} + X_m$,

$X_R = X_{lr} + X_m$,

it becomes:

$$Z_S^+ = (R_S + p X_{ls}) + \frac{p X_m \left(\dfrac{R_r}{\left(1 - j\dfrac{\nu}{p}\right)} + p X_{lr}\right)}{\left(\dfrac{R_r}{\left(1 - j\dfrac{\nu}{p}\right)} + p X_{lr}\right) + p X_m},$$

which can be represented by the equivalent circuit shown in fig. 3.

From fig. 3, the voltage equation in terms of the positive sequence operational impedance Z_s^+ is:

$$V_s^+ = Z_s^+ I_s^+ , \qquad (5)$$

For the negative sequence:

$$V_s^- = Z_s^- I_s^- . \qquad (6)$$

The negative sequence circuit is the same as the positive sequence circuit shown in fig. 3 with j replaced by $-j$. It should be noted that the effect of frequency on the rotor resistance for negative sequence might be incorporated easily into the mathematical model if the resistance/frequency characteristic is known.

The developed electromagnetic torque in terms of sequence quantities may be expressed as:

$$T_e = j\,(X_m/\omega_m)\,I^+_r\,I_s - I^+_s\,I_r) \,. \quad (7)$$

Where ω_m is the synchronous speed in mechanical radians/sec [11].

In this analysis, saturation, core losses and skin effect have been ignored. All machine parameters are assumed constant.

2.1. Delta-connected motor

For the delta-connected motor shown in fig. 2-a, the terminal constraints are:

$$V - V_{sa} = 0,$$

$$V_{sc} + \frac{X_c}{p}\,(I_{sc} - I_{sb}) = 0\,, \quad (8)$$

where

$$X_c = 1/\omega C\,.$$

Writing the winding voltages and currents in terms of their instantaneous symmetrical components as given by eq. (2), eq. (8) becomes:

$$V = \frac{1}{3}\,(V^+_s + V^-_s)\,,$$

$$0 = \frac{1}{3}(av^+_s + a^2V^-_s) + j\frac{X_c}{p}(I^+_s - I^-_s)\,. \quad (9)$$

Using eqs. (5) and (6), and the operational equivalent circuit of fig. 2, eq. (9) can be written as:

$$V = \frac{1}{\sqrt{3}}[(R_s + X_s p)I^+_s + X_m pI^+_r + (R_s + X_s\,p)\,I^-_s + X_m\,pI^-_r\,,$$

$$0 = \left[\frac{R_r}{1 - j\frac{\nu}{p}} + X_r p\right] I_r^+ + X_m pI^+_s\,,$$

$$0 = \left[\frac{R_r}{1 + j\frac{\nu}{p}} + X_r p\right] I_r^- + X_m pI^-_s\,,$$

$$0 = \frac{1}{\sqrt{3}}[a\{(R_s + X_s p)I^+_s + X_m pI^+_r\} + a^2\{(R_s + X_s\,p)I^-_s + X_m pI^-_r\}] + j\frac{X_c}{p}(I^+_s - I^-_s)\,. \quad (10)$$

The instantaneous symmetrical components of I_s and I_r being complex, they can be written in terms of their real and imaginary parts as:

$$\begin{aligned} I^+_s &= I_{sx} + jI_{sy} \\ I^-_s &= I_{sx} - jI_{sy} \\ I^+_r &= I_{rx} + jI_{ry} \\ I^-_r &= I_{rx} - jI_{ry} \end{aligned} \quad (11)$$

Substituting eq. (11) into eq. (7), the developed torque can be written as:

$$T_e = 2X_m(I_{rx}I_{sy} - I_{sx}I_{ry})\,. \quad (12)$$

Substituting eq. (11) into eq. (10) we get:

$$p[I] = [X]^{-1}[V]\,. \quad (13)$$

Where:

$$[I] = [I_{sx} \quad I_{sy} \quad I_{rx} \quad I_{ry}]^T\,, \quad (14)$$

$$[X] = \begin{bmatrix} \frac{2}{\sqrt{3}}X_s & 0 & \frac{2}{\sqrt{3}}X_m & 0 \\ X_m & 0 & X_r & 0 \\ 0 & X_m & 0 & X_r \\ \frac{1}{\sqrt{3}}X_s & X_s & \frac{1}{\sqrt{3}}X_m & X_m \end{bmatrix}\,, \quad (15)$$

$$[V]=\begin{bmatrix} V-\frac{2}{\sqrt{3}}R_sI_{sx} \\ -R_rI_{rx}-\upsilon X_rI_{ry}-\upsilon X_mI_{sy} \\ -R_rI_{ry}+\upsilon X_rI_{rx}+\upsilon X_mI_{sx} \\ -\frac{1}{\sqrt{3}}R_sI_{sx}-R_sI_{sy}-2X_cq_{sy} \end{bmatrix}, \quad (16)$$

$$q_{sy}=I_{sy}/p \text{ ; or } pq_{sy}=I_{sy}. \quad (17)$$

2.2. Star-connected motor

For the star-connected motor shown in fig. 2-b, the terminal constraints are:

$$V-V_{sa}+V_{sb}=0,$$

$$V_{sa}-\frac{X_c}{p}I_{sc}-V_{sc}=0. \quad (18)$$

Using the previous procedures the matrix [*X*] and the array [*V*] of eqs. (15) and (16) are now:

$$[X]=\begin{bmatrix} \sqrt{3}X_s & -X_s & \sqrt{3}X_m & -X_m \\ X_m & 0 & X_r & 0 \\ 0 & X_m & 0 & X_r \\ \sqrt{3}X_s & X_s & \sqrt{3}X_m & X_m \end{bmatrix}, \quad (19)$$

$$[V]=\begin{bmatrix} V-\sqrt{3}R_sI_{sx}+R_sI_{sy} \\ -R_rI_{rx}-\upsilon X_rI_{ry}-\upsilon X_mI_{sy} \\ -R_rI_{ry}+\upsilon X_rI_{rx}+\upsilon X_mI_{sx} \\ -\sqrt{3}R_sI_{sx}-R_sI_{sy}-\frac{1}{\sqrt{3}}X_cq_{sx}+X_cq_{sy} \end{bmatrix}, \quad (20)$$

$$q_{sx}=I_{sx}/p \text{ ;or } pq_{sx}=I_{sx}. \quad (21)$$

3. Experimental setup

A method is introduced to control the speed of single-phase induction motors by changing both the frequency and amplitude of the applied voltage on the motor. This strategy needs generating control pulses synchronized with the supply. A power switch, such as triac, is used as shown in fig. 4. This method is simple, inexpensive and reliable. The firing circuit fulfills two requirements:

1. Changing the frequency of the applied voltage to the motor (integral-cycle control).
2. Changing the amplitude of the applied voltage to the motor (phase angle control).

To fulfill these requirements we need the following circuits:

- Zero Voltage Crossing Detector (ZVCD) that detects the zero voltage point which is the start of measuring the firing angle α. This circuit is common to both phase control and integral-cycle control circuits. Fig. 5 shows this circuit.
- Ring-tail counter circuit (Johnson counter) which changes the firing signal according to the required frequency (integral-cycle control circuit). Fig. 6 shows this circuit. The input to this circuit is the output signal from the ZVCD circuit. Fig. 7 shows the output of the circuit, according to the required frequency, to fire the triac.
- Delay circuit which initiates the pulse after the firing angle α (phase control circuit). Fig. 8 shows the circuit used. The firing angle is counted starting from ZVCD circuit output pulse. It is generated in digital form. The PLC outs 4 bits containing the required delay, which is latched in the appropriate latch. At

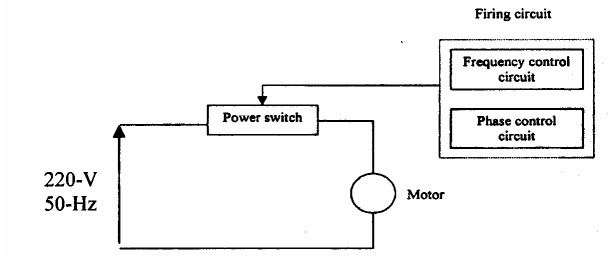

Fig. 4. Block diagram for the proposed drive.

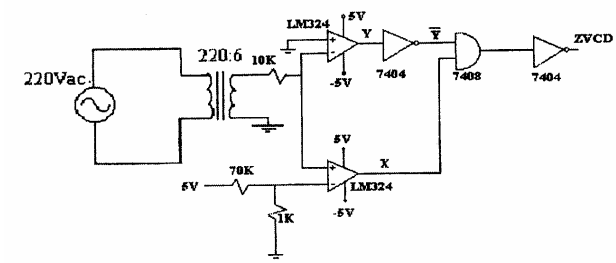

Fig. 5. Zero voltage crossing detection circuit.

the beginning of each half-cycle of supply, which is marked by the ZVCD circuit, the counter is loaded by the desired delay from the latch IC-74273 output. The counter begins to count down, then a pulse is taken from the borrow out pin of counter IC-74193. Both the counter and the D-type flip flop IC's operates on a clock signal, which comes from the oscillator circuit.

- Oscillator circuit as a clock signal. Fig. 9 shows the circuit used. In order to fire the triac at any firing angle, the half cycle is divided into 16 parts so the resolution is $180^o/16 = 11.25^o$. The counter should count 16 times in 10-ms. This means that the counter clock frequency should be 16/0.01 = 1.6-kHz. This oscillator is realized using the NE-555 timer.
- Pulse conditioning circuit, which is used for conditioning the firing pulses of the triac and send it to the triac gate after being amplified. Fig. 10 shows the circuit used. In this circuit the D-type flip-flop 7474 is used to give the adequate pulse duration and the pulse synchronized with the clock pulses. The n-p-n transistor is used to amplify the pulse sent to the triac gate.

4. Experimental results

A systematic experimental investigation is undertaken to evaluate the effectiveness of the proposed speed control scheme.

4.1. Delta-connected motor

Fig. 11 shows speed response at no-load for four speeds for the delta-connected motor. The speed response corresponds to the fundamental frequencies f/3, f/4, f/5 and f/7, where f is the supply frequency (f = 50-Hz).

Fig. 12-a shows the speed response for a load of 1-Nm for f/3. The speed drops due to loading by 9% and the starting time increases by 30%. Fig. 12-b shows the applied voltage to the motor and the drawn current.

Fig. 13-a shows the speed response for a load of 1-Nm for f/7. The speed drops due to loading by 35% and the starting time increases by 25%. Fig. 13-b shows the applied voltage to the motor and the drawn current.

The voltage control by increasing the firing angle can be noticed in fig. 13-b. Also, it should be noticed that, at the intervals of current discontinuity an induced voltage is observed for both f/3 and f/7 having the fundamental frequency.

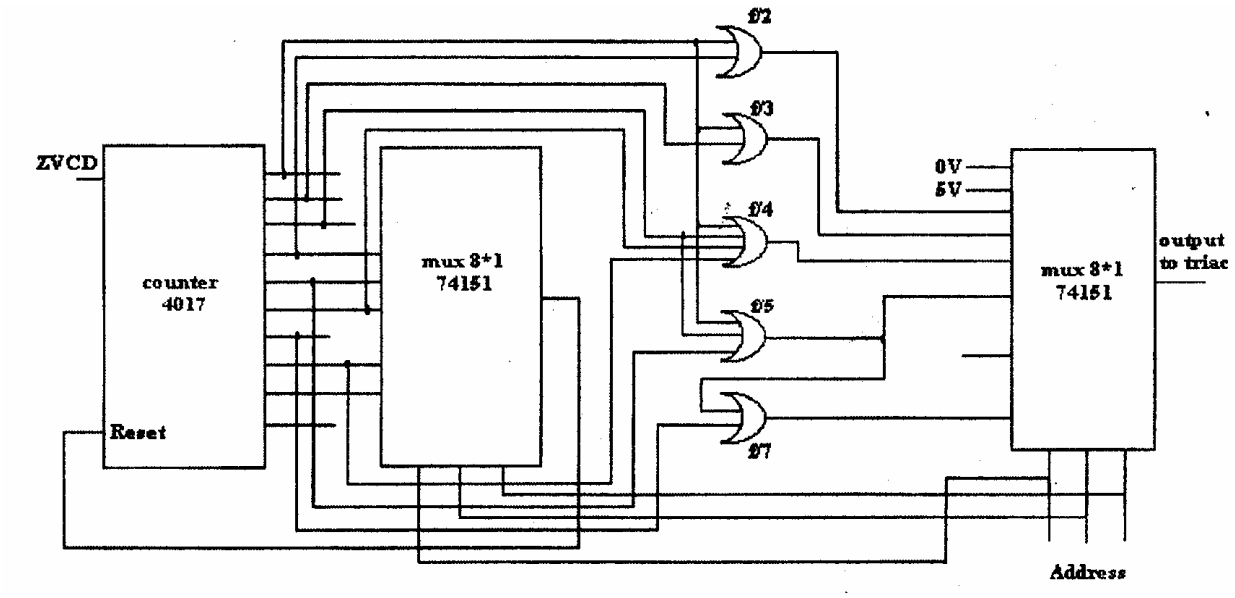

Fig. 6. Ring-tail counter circuit.

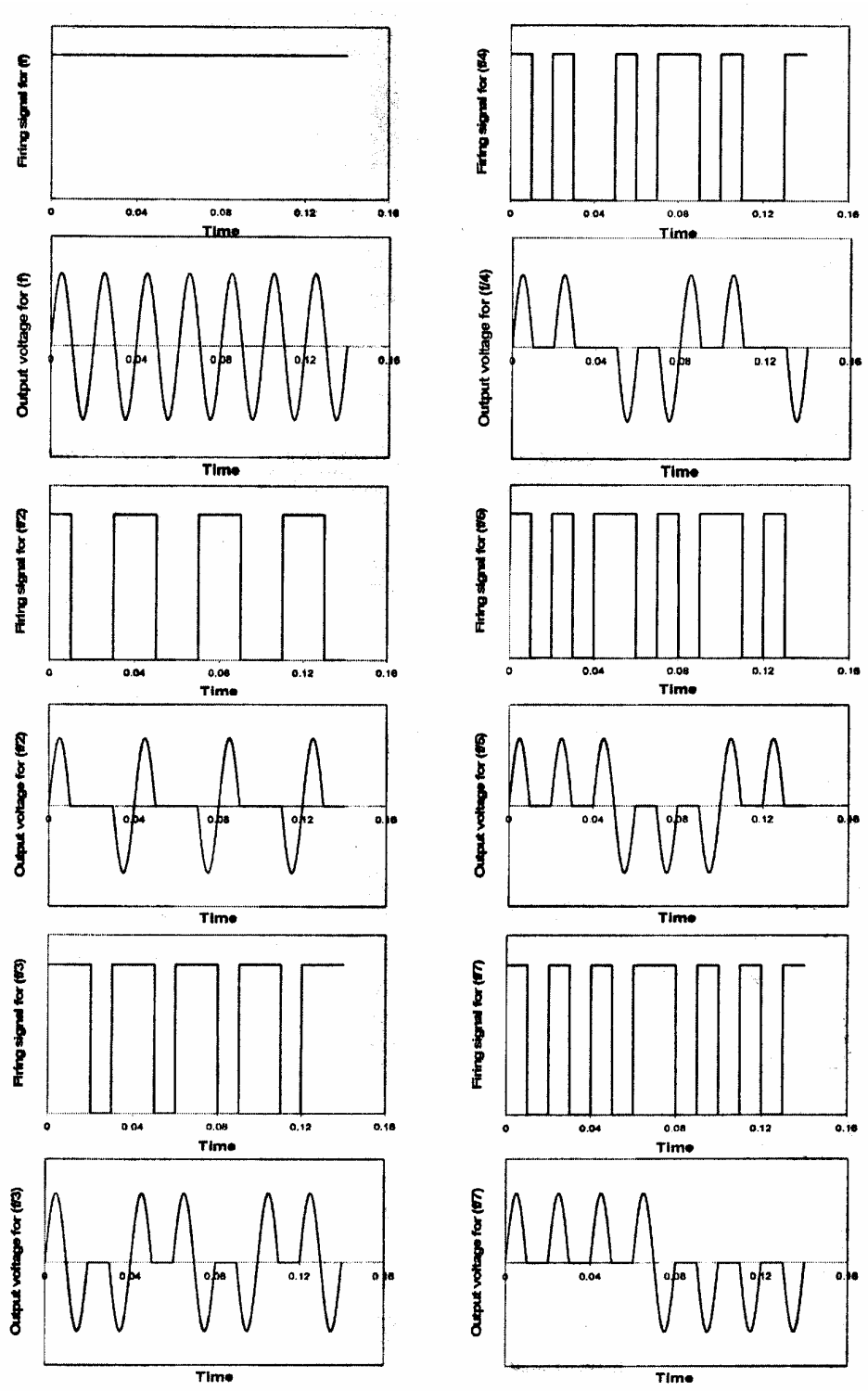

Fig. 7. Firing signal and output voltage at different required frequencies for resistive load with delay angle $\alpha = 0$.

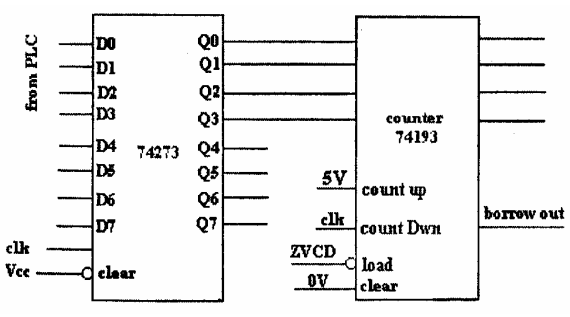

Fig. 8. The delay circuit.

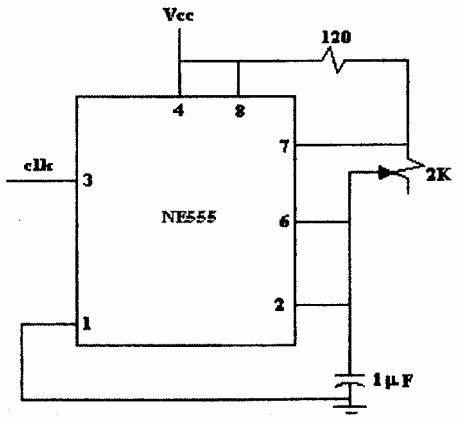

Fig. 9. The oscillator circuit.

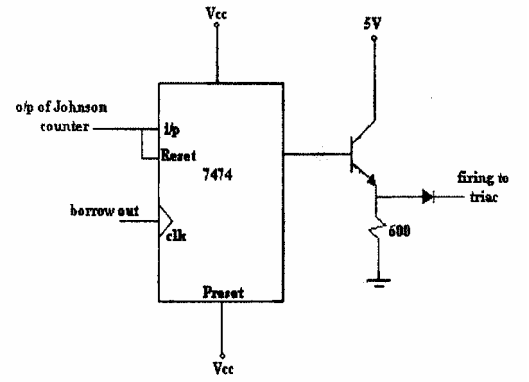

Fig. 10. The pulse conditioning circuit.

4.2. Star-connected motor

Fig. 14 shows the speed response at no-load for f/3, f/4, f/5 and f/7. Comparing fig. 14 with fig. 11 reveals that the starting time of the motor is larger for star-connected motor than that for delta-connected motor. This is attributed to the reduced phase voltage for the star-connected stator.

Fig. 15-a shows the speed response for a load of 1-Nm corresponding to f/5. The speed drops due to loading by 12%. Fig. 15-b shows the applied voltage to the motor and the drawn current when the motor is loaded with 1-Nm.

Fig. 16-a shows the speed response for a load of 1-Nm corresponding to f/7. The speed drops due to loading by 14%. Fig. 16-b shows the applied voltage to the motor and the drawn current when the motor is loaded with 1-Nm.

The voltage control by increasing the firing angle can be noticed in both f/5 and f/7. Also, it should be noticed that, at the intervals of current discontinuity an induced voltage is observed having the fundamental frequency.

The main disadvantage of the proposed speed control technique, when compared to the much more expensive inverter drives, is the pronounced harmonic distortion in the drawn current. In order to assess the harmonic distortion an experimental spectral analysis was performed. Fig. 17 shows the spectral analysis for the stator current for f/3, f/4, f/5 and f/7. Although higher frequency harmonics appear in the spectral analysis, the rotor runs at a speed corresponding to the fundamental frequency. This is mainly due to the low-pass filter effect of the mechanical time constant of the motor, which shows its corner frequency at a low frequency.

5. Simulation results

Fig. 18 shows the simulation results for the star-connected motor for f/5. Fig.18-a shows no-load speed response. Fig. 18-b shows the stator current for a load of 1-Nm. Fig. 18-a and fig.18-b are comparable to fig.14 for f/5 and fig. 15-b, respectively.

6. Conclusions

This paper presents a new scheme for multi-speed operation of a single-phase induction motor. The scheme is simple, cheap and reliable. Its performance is not comparable to an inverter; as it is not able to provide continuous speed control. It can only provide

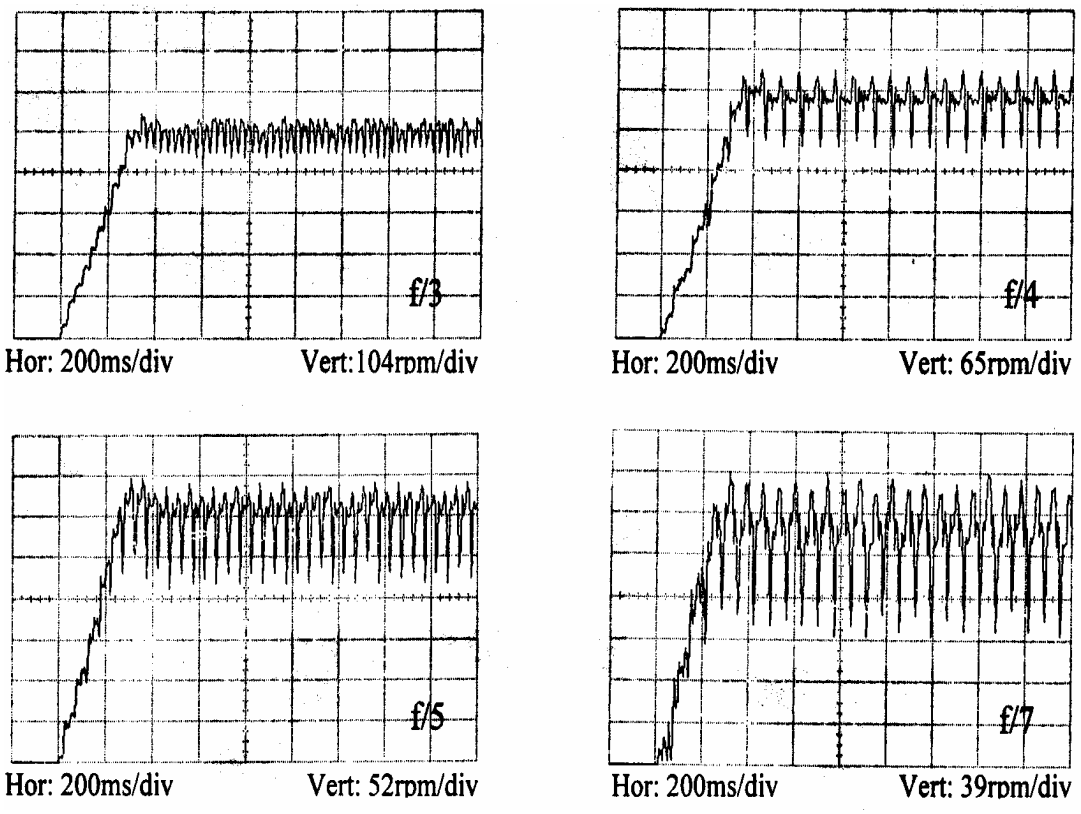

Fig. 11. Different speed response at no-load for different fundamental frequencies for delta-connected motor.

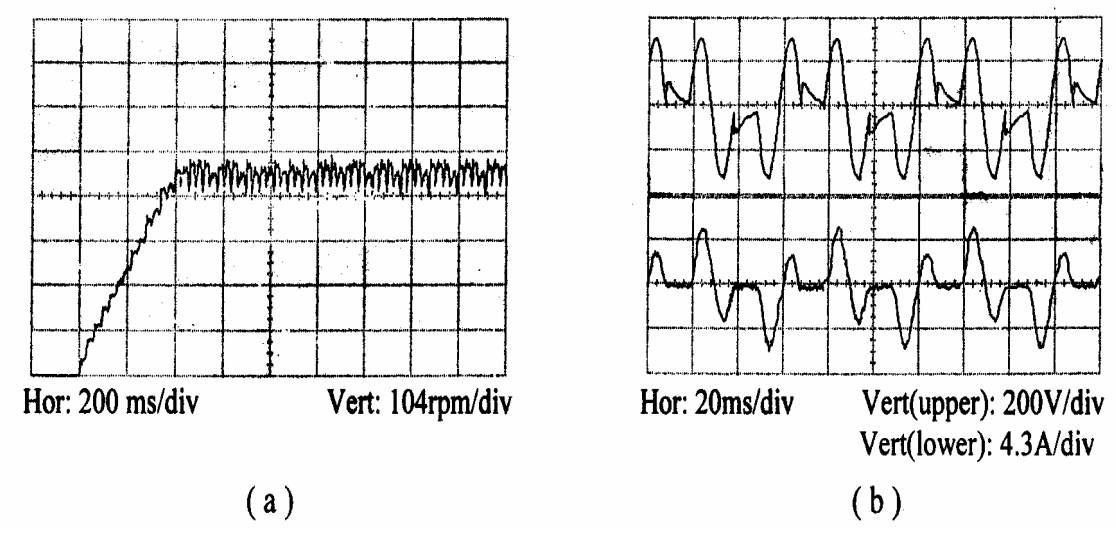

Fig. 12. Speed response, applied voltage to motor and drawn current corresponding to a load of 1-Nm for f/3.

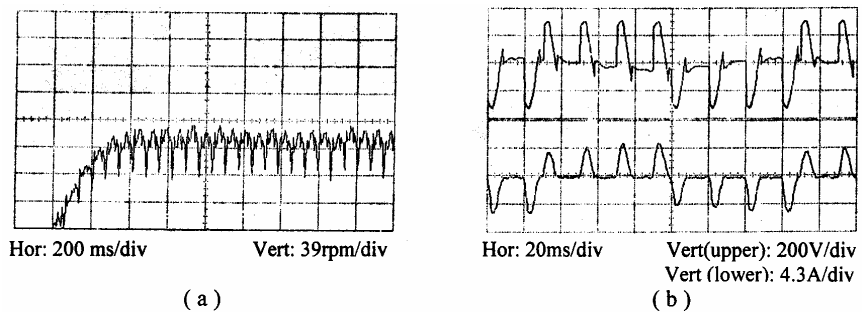

Fig. 13. Speed response, applied voltage to motor and drawn current corresponding to a load of 1-Nm for f/7.

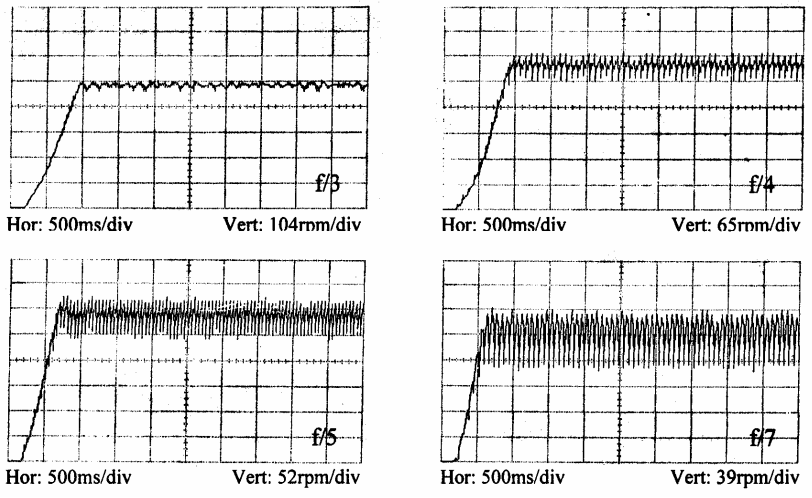

Fig. 14. Different speed response at no load for different fundamental frequencies for star-connected motor.

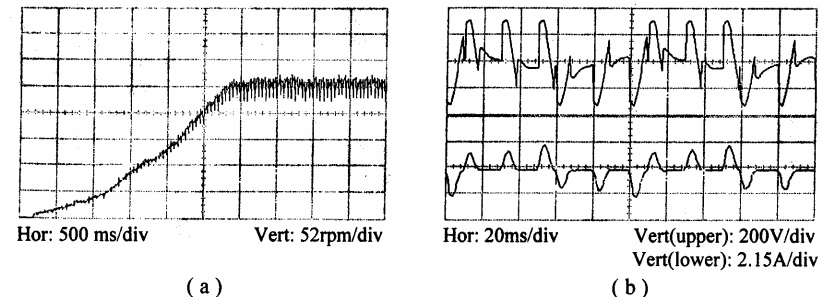

Fig. 15. Speed response applied voltage to motor and drawn current corresponding to a load of 1-Nm for f/5.

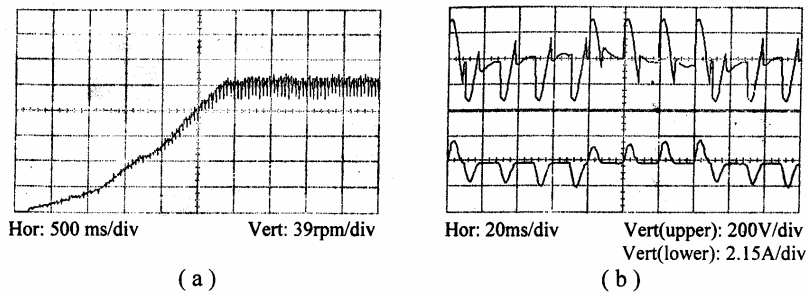

Fig. 16. Speed response, applied voltage to motor and drawn current corresponding to a load of 1-Nm for f/7.

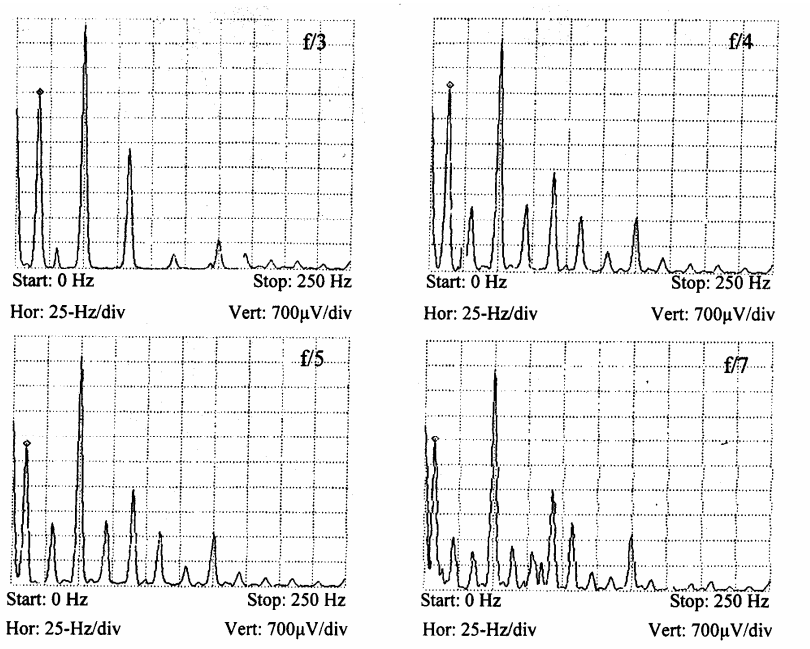

Fig. 17. Spectral analysis of stator current at different fundamental frequencies.

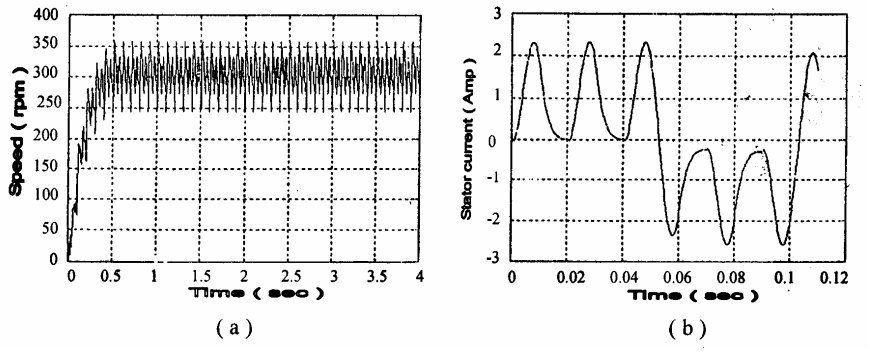

Fig. 18. Simulation results for star-connected motor for f/5.

discrete multi-speed operation. On the other hand, the circuit topology of the proposed scheme is quite simple, as it comprises only a single naturally commutated device, a triac. Theoretical and experimental study provided substantial evidence that the scheme can provide a wide variety of speeds. This can be achieved by controlling the fundamental frequency of the supply. This was achieved using ring-tail counter circuit which implements integral-cycle control technique. Moreover, it provides, also, the facility of phase control to keep the voltage/frequency ratio constant. However, low frequencies are accompanied by remarkable speed ripples. These ripples are due to the harmonics, which can be observed in the stator current spectrum analysis. Although higher frequency harmonics appear in the spectral analysis, the rotor runs at a speed corresponding to the fundamental frequency. This is mainly due to the low-pass filter effect of the mechanical time constant of the motor, which shows its corner frequency at a low frequency.

Appendix A

The machine used is a three-phase, squirrel-cage, induction motor, 380-V, star-connected, 0.52-A, 175-W, 50-Hz, 4-pole,

1360-rpm. The machine parameters are as follows :

R_s = 48.56 Ω, L_{ls} = 0.175 H,
R_r = 26.65 Ω, L_{lr} = 0.175 H,
L_m = 3.0 H.

Moment of inertia $J = 1.24 \times 10^{-4}$ Kg.m^2,
Viscous coefficient $B = 1.435 \times 10^{-5}$ N.m./rad/sec.
Starting and running capacitor for delta-connected motor $C = 40\ \mu F$.
Starting and running capacitor for star-connected motor $C = 80\ \mu F$.

References

[1] T. A. Lipo, "The Analysis of Induction Motors With Voltage Control by Symmetrically Triggered Thyristors," IEEE Trans. on Power Apparatus and Systems, Vol. PAS-90 (2), pp. 515-525 (1971).

[2] D.E. Cattermole, R.M. Davis, and A.K. Wallace, "The Design Optimization of a Split-Phase Fan Motors With Triac Voltage (Speed) Control," IEEE Trans. on Power Apparatus and Systems, Vol. PAS-94 (3), pp. 778-785 (1975).

[3] D.E. Cattermole and R.M. Davis, "Triac Voltage (Speed) Control For Improved Performance of Split-Phase Fan Motors," IEEE Trans. on Power Apparatus and Systems, Vol. PAS-94 (3), pp. 786-791 (1975).

[4] M. A. Abdel-Halim, "Solid-State controlled Single-Phase Induction Motor," Electric Machines and Power Systems Journal, Vol. 24 (6), pp. 623-638 (1996).

[5] M.A. Abdel-Halim, "Control of Single Phase Induction Motor Using Forced-Commutated Electronic Switches," Electric Machines and Power Systems Journal, Vol. 25 (12), pp. 1119-1133 (1997).

[6] A.A.M. Makky, Gamal M. Abdel-Rahim, and Nabil Abd El-Latif, "A Novel DC Chopper Drive for a Single-Phase Induction Motor," IEEE Trans. on Industrial Electronics, Vol. 42 (1), pp. 33-39 (1995).

[7] G. Choe, A.K. Wallace, and M. Park, "An Improved PWM Technique for ac Choppers," IEEE Trans. on Power Electronics, Vol. 4 (4), pp. 496-505 (1989).

[8] D. Jang, and J. Won, "Voltage, Frequency, and Phase-Difference Angle Control of PWM Inverters-Fed Two-Phase Induction Motors," IEEE Trans. on Power Electronics, Vol. 9 (4), pp. 377-383 (1994).

[9] D. Jang, G. Choe, and M. Ehsani, "Asymmetrical PWM Technique with Harmonic Elimination and Power Factor Control in ac Choppers," IEEE Trans. on Power Electronics, Vol. 10 (2), pp. 175-184 (1995).

[10] M. B. R. Correa, C. B. Jacobina, A. M. N. Lima, E.R.C. Lima, and E.R.C. da Silva, "Rotor-Flux-Oriented Control of a Single-Phase Induction Motor Drive," IEEE Trans. on Industrial Electronics, Vol. 47 (4), pp. 832-841 (2000).

[11] S. S. Murthy, Bhim Singh and A.K. Tandon, "Dynamic Models for the transient Analysis of Induction Machines with Symmetrical Connections," Electric Machines and Electromechanics, Vol. 6 (6), pp. 479-492 (1981).

Received February 4, 2003
Accepted May 25, 2003